Robust Planning of Power System Decarbonization Pathways Considering Demand Response

Haiyue Yu, Yusheng Xue, Minglei Bao, Hengyu Hui, Dongliang Xie, and Yi Ding, *Member*, *IEEE*

Abstract—**Power systems are undergoing a policy-driven transition to decarbonization, which increases uncertainty and fluctuation due to the high penetration of renewable energy. Concurrently, advancements in communication and control technologies are unlocking greater demand-side flexibility. However, existing conventional long-term resource planning models for power systems do not adequately integrate demand response (DR) resources, operation simulations that account for uncertainty, and social factors such as government policy. To address these shortcomings, this paper introduces a robust planning framework for power system decarbonization pathways, specifically considering DR load as a critical flexible resource along with other techniques and impacting factors. Firstly, the long-term impacts of government policies and other social factors on system resource investment costs and development constraints are quantitatively considered, and the adjustable and transferable DR loads as key flexible resources are incorporated to smooth the fluctuations caused by renewable energy generation. Then, a three-stage robust planning model is developed by integrating long-term development planning, day-ahead unit commitment simulation, and intra-day power dispatch simulation to obtain the optimal solution with the lowest total cost over the planning period. Moreover, the column and constraint generation algorithm is modified to solve the planning model, specifically designed to address the decision-dependent uncertainty arising from new asset investments. Case study based on a provincial power system shows that the proposed framework enhances the integration of renewable energy by applying DR resources in line with real social development trends. The combination of long-term system planning, refined short-term operation simulation, and strategic DR integration ensures that the resulting decarbonization pathway is not only economically feasible but also highly robust and reliable.**

Index Terms—**Power system decarbonization, social factor, demand response, renewable energy, flexibility, cyber−physical−social system (CPSS), robust planning.**

Manuscript received: March 26, 2025; revised: August 29, 2025; accepted: November 2, 2025. Date of CrossCheck: November 2, 2025. Date of online publication: November 13, 2025.

This work was supported by the Basic Research Program of Jiangsu Province (No. BK20232026), the National Science Foundation for Distinguished Young Scholars of China (No. 52125702), and the Science and Technology Project of NARI Technology Co., Ltd. (No. GF-GFWD-210338).

H. Yu, M. Bao, H. Hui, and Y. Ding (corresponding author) are with the College of Electrical Engineering, Zhejiang University, Hangzhou 310027, China (e-mail: yuhaiyue@zju.edu.cn; baominglei@zju.edu.cn; huihengyu@zju.edu.cn; yiding@zju.edu.cn).

Y. Xue (corresponding author) and D. Xie are with the State Grid Electric Power Research Institute (NARI Group Corporation), Nanjing 211106, China (e-mail: xueyusheng@sgepri.sgcc.com.cn; xiedongliang@sgepri.sgcc.com.cn).

DOI: 10.35833/MPCE.2025.000134

I. Introduction

The global imperative to mitigate climate change driven by carbon emissions has spurred many nations to establish ambitious reduction targets [1]. China has committed to achieving peak carbon emissions by 2030 and carbon neutrality by 2060 [2]. The power sector is central to this effort [3], making the scientific planning of its decarbonization pathway critical.

Studies on power system resource planning have been conducted since the inception of power systems. The power system is a cyber−physical−social system (CPSS), deeply influenced by the social system [4]. However, the existing research has not effectively integrated the impact of social factors on long-term planning, which may result in solutions that deviate from social development. In terms of planning objects, early studies focused on traditional generators, but the trend of decarbonization has shifted the focus to renewable energy generation [5]. Expanding renewable energy is essential but also brings operation challenges, including uncertainty and fluctuation, and a temporal mismatch with loads [6]. Therefore, new flexible resources are needed as the penetration of renewable energy increases.

Energy storage facilities are one solution to provide flexibility, and some studies have incorporated them into planning [7]. However, their large-scale application faces problems like high costs, short service life, and operation safety risks. Thus, more economical and reliable regulation resources beyond energy storage are needed. With advances in technology, more load resources have become controllable [8]. Demand response (DR) technology plays a positive role in handling renewable energy fluctuations [9] and has advantages like low investment costs compared with energy storage [10]. While some studies propose considering demand-side resources [11], most current planning models do not adequately account for the flexibility of DR or treat its capacity as a planned variable resource [12].

In terms of planning models, early studies relied on cost-minimization and supply-demand balance constraints [13], [14]. Facing the low-carbon transition, studies now convert carbon emissions into costs [15] or include them as constraints [16], [17]. Moreover, the high penetration of renewable energy causes significant fluctuations, making simple capacity balance constraints insufficient, thus requiring development schemes to consider the volatile operation conditions [18]. Studies have developed bi-level planning models incorporating operation simulation [19], [20], with an upper planning level and a lower operation level, usually aiming at minimizing the total cost [21]. While the annual chronological simulation is computationally expensive, optimizing for typical periods is more cost-effective [22]. Unit commitment (UC) optimization is critical due to fluctuations but is often not explicitly integrated into long-term planning [23]. Without UC optimization, the planning feasibility area shrinks [24], so UC must be considered in operation simulations [25].

Stochastic optimization and robust optimization are widely used for addressing uncertainty [26]. Stochastic optimization often requires sampling many scenarios, which needs extensive data and computational resources [18]. In contrast, the robust optimization only needs uncertainty intervals and finds the optimal objective in the worst-case scenario, providing more adaptable results [27]. Common solution algorithms include Benders decomposition or column and constraint generation (CCG) algorithms [28]. However, these algorithms are not well suited for decision-dependent uncertainty and require further study [29].

To fill these gaps, this paper proposes a robust planning framework for power system decarbonization pathways, aiming to obtain the optimal development options for generation, storage, and DR loads over the long term. The main contributions of this study are as follows.

1) A novel robust planning framework for power system decarbonization pathway is constructed. This framework quantitatively assesses the long-term impacts of social factors on system resource investment costs and development constraints. It also incorporates adjustable and transferable DR loads as flexible resources to mitigate fluctuations in renewable energy generation, and the capacity of DR loads is treated as an expandable variable like other resources.

2) A three-stage robust planning model is proposed. This model integrates long-term development planning, day-ahead UC simulation, and intra-day power dispatch simulation. The robust optimization is adopted to address uncertainties to obtain the most cost-effective and adaptable development plan. Meanwhile, a modified column and constraint generation (MCCG) algorithm capable of handling decision-dependent uncertainty is proposed for solving the planning model.

II. Robust Planning Framework of Power System Decarbonization Pathway

In this section, a robust planning framework for power system decarbonization pathway is innovatively constructed from a perspective of CPSS, as shown in Fig. 1. The resources covered in this framework include generation resources, energy storage resources, external power supply, and DR loads. The impact of social factors and the uncertainty of photovoltaic (PV) power, wind power, and external power input during the system operation on long-term planning are considered. The above elements are finally integrated into a three-stage robust planning model to obtain the resource development plan.

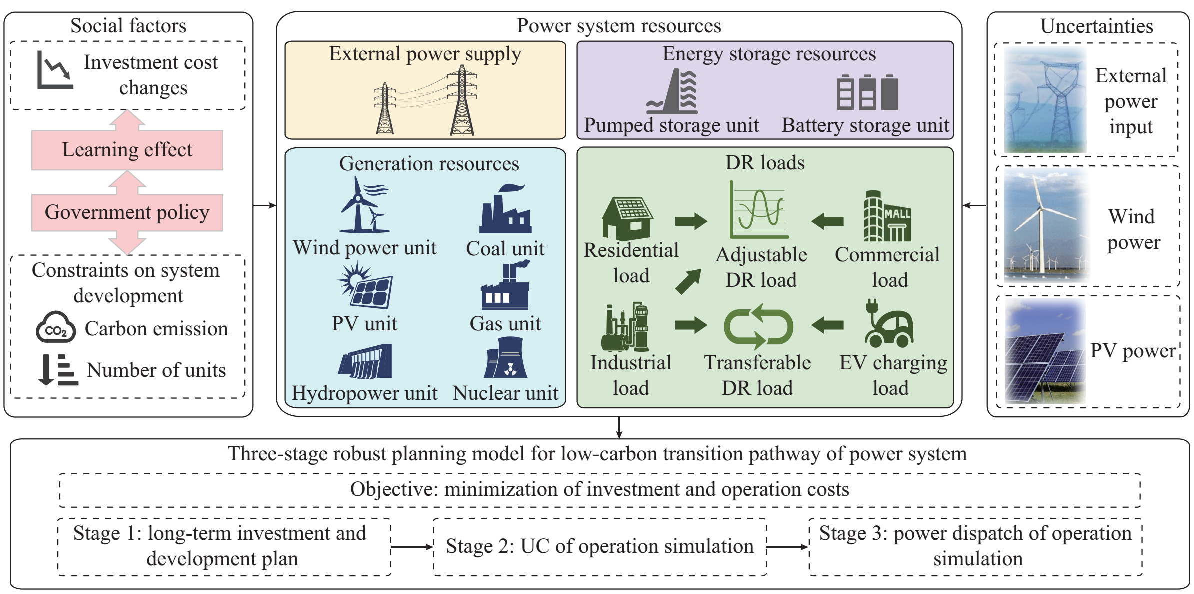

Fig. 1. Robust planning framework for power system decarbonization pathway.

A. Power System Resources

Generation resources considered in the proposed framework include coal units, gas units, nuclear units, wind power units, PV units, and hydropower units. Energy storage resources include pumped storage units and battery storage units. In the context of multi-region power system interconnections, the external power supply is also considered in the proposed framework. DR loads are highlighted in the proposed framework. Based on social attributes, loads are divided into residential loads, commercial loads, industrial loads, and electric vehicle (EV) charging loads. Generally, they all have two parts, which are fixed power part and responsive power part. Based on response characteristics, the responsive power part is divided into adjustable and transferable DR loads. Residential and commercial loads are mainly air-conditioning loads. They can be reduced over a period of time without restoration, so they are adjustable DR loads. Industrial loads include production loads and non-production loads. The total production volume of a factory needs to be kept constant over a period of time, and the reduced production at one time point must be made up at another time point in the time period. The production load power is strongly correlated with the production volume, so the production loads are considered as transferable loads. Non-production loads are loads such as air conditioning inside the factory, and they are considered as adjustable DR loads. EV users have a rigid demand for electricity and a flexible demand for charging time, therefore EV charging loads are transferable DR loads.

B. Social Factors

Since power system is inherently a CPSS, during the system evolution, it is necessary to consider the impact of social factors on various types of resources [4]. The integration of social factors offers added value to the planning framework by providing a more holistic and realistic representation of the power system evolution. This paper specifically considers the influence of social factors on system planning from two critical aspects: investment cost changes and constraints on system development.

1) Investment Cost Changes

This paper employs the learning effect to depict the long-term investment cost changes of various types of resources. As an economic term, the learning effect refers to the reduction in production cost as the output increases. The essence of this phenomenon lies in the learning ability of human beings in the continuous production process. Experience is continuously accumulated in the production process, which in turn drives the technological progress. The pace of this process is influenced by social factors like social knowledge, management skills, and government policies [30]. For resources in the power system, according to [31]-[33], the investment cost per unit capacity of the resource C varies with the cumulative installed capacity E, which can be expressed as:

$$C = C_0 E^{\log_2(1-LR)} \tag{1}$$

where C_0 is the initial investment cost per unit capacity of the resource; and LR is the learning rate, defined as the decrease rate in investment cost per unit capacity when the cumulative installed capacity is doubled. For example, $LR=$ 20% means that the investment cost per unit capacity decreases by 20% when the cumulative installed capacity is doubled.

Within the same social environment, the social knowledge and management capability are largely comparable. Therefore, the most significant factor influencing learning rates lies in government policies. These policies determine varying degrees of financial subsidies, tax incentives, and intellectual property protection for different technologies, thereby guiding differentiated research and development investments by society and enterprises and influencing their learning rates. Under more proactive policies, the technology learning rates increase, while the investment costs decline more rapidly.

Learning rates are typically obtained by fitting accumulated investment data. Numerous researchers and organizations have calculated learning rates for a wide range of generation resources [31]-[37]. National Renewable Energy Laboratory (NREL) identifies three scenarios for changes in investment cost per unit capacity based on technological development forecasts: advanced, moderate, and conservative scenarios [38]. NREL also provides forecasts for future investment cost changes for almost all types of generation units in these three scenarios. Studies show that the learning rates of various power generation technologies generally range from 0% to 20%. For example, the learning rate of wind power technology is between 5.8% and 11.2% [31], [34], [35], that of PV power technology between 2.2% and 18.4% [32], [35], [36], and that of nuclear power technology between 2% and 15% [33], [37]. However, these studies do not address the learning rate of DR technologies, and the limited historical data make it difficult to derive this rate through extrapolation.

While establishing a direct quantitative formula between policy instruments and learning rates is a complex research field, a scenario-based approach can be used to analyze the impact of different policy-driven cost trajectories. In this paper, the advanced, moderate, and conservative scenarios are defined, which are analogous to the technology forecasting framework used by NREL. The policies in these three scenarios differ in terms of the intensity and proactive nature of their efforts to promote the development of relevant technologies, leading to variations in LR. Based on the empirically observed LR for other energy technologies, a plausible LR range of 5%-15% for DR technology is defined. In the advanced scenario, the government adopts more proactive policies, including more substantial fiscal subsidies and stronger intellectual property protection to facilitate the rapid technological advancement, resulting in a high LR of 15%. The moderate scenario and conservative scenario, corresponding to the general and minimal policy supports, assume LR of 10% and 5%, respectively.

This dynamic cost modeling, as opposed to fixed cost assumptions, provides a more accurate projection of future system economics. Incorporating it into the power system planning framework allows for more realistic outcomes. Meanwhile, by comparing the planning outcomes across different scenarios, the impact of different learning rates on system development can be obtained.

2) Constraints on System Development

As society progresses and the understanding of environmental challenges increases, the development direction and path of power system are continually revised through evolving government policies, thereby creating crucial constraints on its evolution. For instance, in response to global warming, governments implement progressively tighter carbon emission constraints [39]. These policy-driven constraints directly limit the permissible power generation capacity of coal and gas units, decisively affecting the types and scales of units developed in later stages. Incorporating these social factors as development constraints ensures that the proposed framework generates pathways that are not only technically feasible but also compliant with critical environmental targets and long-term social objectives. Moreover, governments engage in advanced planning for certain power capacities such as external power input. This capacity is not treated as a decision variable in planning but serves as a boundary condition. In addition, some governments require renewable energy projects to be coupled with the development of storage unit to ensure output stability, creating coupling constraints between renewable generation capacity and storage capacity.

C. Power Uncertainties

As the penetration of renewable energy continues to rise, the power uncertainties increase. In the proposed framework, the uncertainties of wind power, PV power, and external power input are considered. To avoid the computational complexity associated with large-scale operation scenarios during planning, the robust optimization techniques will be employed in this study. Accordingly, these uncertainties are modeled using a boxed uncertainty set, as shown in (2).

$$P=\hat{P}+\Delta P \quad \Delta P \in \left[\Delta P_{\min}, \Delta P_{\max}\right] \tag{2}$$

where P, $\hat{P}$, and ΔP are the actual value, predicted value, and uncertainty deviation, respectively; and $\Delta P_{\max}$ and $\Delta P_{\min}$ are the maximum and minimum values of this uncertainty deviation, respectively.

For this portion of uncertainty, the proposed framework addresses it through robust optimization. Beyond this, uncertainties such as equipment failures also require measures to be taken. The proposed framework incorporates an operation reserve capacity within the power system to cope with them.

III. Three-stage Robust Planning Model for Low-carbon Transition Pathway of Power System

To cope with the greater uncertainties arising from increased renewable energy sources in the future, the planning should be as adaptive as possible to worst-case scenarios. Therefore, a three-stage robust planning model is proposed to address uncertainty for the proposed framework, as shown in Fig. 2. This model consists of one stage for the investment and development plan and two stages for operation simulation, aiming to develop a resource development plan that ensures safe, economical, and stable system operation even under the worst uncertainties through robust optimization.

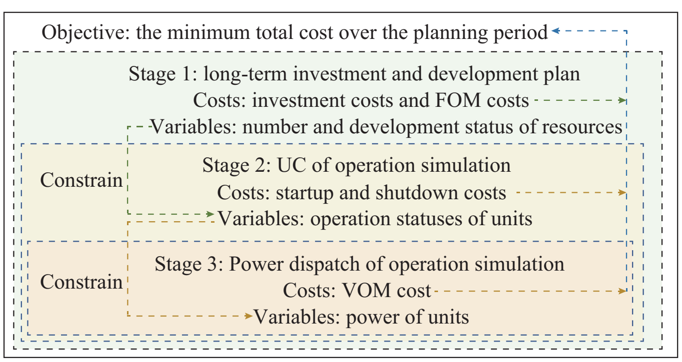

Fig. 2. Three-stage robust planning model.

A. Stage 1: Long-term Investment and Development Plan

In Stage 1, the long-term investment and development plan for resources is developed on a yearly time scale. The variables involved in this stage are the number of resources to be developed and the development status of them in each year. The costs incurred in this stage C_{S1} include the investment costs and fixed operation and maintenance (FOM) costs, expressed as:

$$C_{S1}=C_{INV}+C_{FOM} \tag{3}$$

where C_{INV} and C_{FOM} are the investment cost and FOM cost, respectively.

The investment cost C_{INV} is calculated as:

$$\begin{aligned} C_{INV} &= \sum_{y=1}^{N_y}\sum_{\Phi \in \Omega_1}\sum_{i \in \Phi}\gamma_y c_{i,y}^{inv} P_i\left(X_{i,y}-X_{i,y-1}\right) \\ \Omega_1 &= \left\{\mathbb{N}_C, \mathbb{N}_G, \mathbb{N}_N, \mathbb{N}_H, \mathbb{N}_W, \mathbb{N}_P, \mathbb{N}_S, \mathbb{N}_D\right\} \end{aligned} \tag{4}$$

where N_y is the total number of years in the planning period; $\mathbb{N}_C$, $\mathbb{N}_G$, $\mathbb{N}_N$, $\mathbb{N}_H$, $\mathbb{N}_W$, $\mathbb{N}_P$, $\mathbb{N}_S$, and $\mathbb{N}_D$ are the type sets of coal units, gas units, nuclear units, hydropower units, wind power units, PV units, energy storage resources, and DR resources to be developed, respectively; Φ is the set of type i resource; $c_{i,y}^{inv}$ is the investment cost per unit capacity of type i resource to be developed in year y; P_i is the rated capacity of type i resource to be developed; $X_{i,y}$ is the number of type i resources to be developed in year y; and γ_y is the capital discount factor in year y, calculated as:

$$\gamma_y=\frac{1}{1+r^y} \tag{5}$$

where r is the annual interest rate.

Considering the influence of learning effects on costs, it can be observed from (1) that $c_{i,y}^{inv}$ is not a constant. It varies over time from year to year and can be expressed as:

$$c_{i,y}^{inv}=c_{i,0}^{inv}\Delta c_{i,y} \tag{6}$$

where $c_{i,0}^{inv}$ is the initial cost per unit capacity of type i resource at the beginning of the planning period; and $\Delta c_{i,y}$ is the cost change rate of type i resource caused by the learning effect in year y.

The FOM cost C_{FOM} is calculated as:

$$C_{FOM}=\sum_{y=1}^{N_y}\sum_{\Phi \in \Omega_1}\sum_{i \in \Phi}\gamma_y c_i^{FOM} P_i X_{i,y} \tag{7}$$

where c_i^{FOM} is the FOM cost per unit capacity of type i resource.

In Stage 1, all resources have a limited number that can be developed in each year and are usually determined by government policies. The constraints on the number of resources are denoted as:

$$X_{i,y,\min} \le X_{i,y} \le X_{i,y,\max} \quad \forall i \in \Phi, \Phi \in \Omega_1, y \in \left\{1,2,\dots,N_y\right\} \tag{8}$$

where $X_{i,y,\max}$ and $X_{i,y,\min}$ are the upper and lower limits of $X_{i,y}$, respectively. The total cumulative number of new resources must follow the principle of being equal to or greater than that in the previous year, so the following constraints on the number of resources exist in adjacent years.

$$X_{i,y+1} \ge X_{i,y} \quad \forall i \in \Phi, \Phi \in \Omega_1, y \in \left\{1,2,\dots,N_y-1\right\} \tag{9}$$

In addition, the following relationship exists between $X_{i,y}$ and the development status $S_{y,i,j}$ of the j^{th} type i resource in year y:

$$X_{i,y}=\sum_{j=1}^{N_i}S_{y,i,j} \quad \forall i \in \Phi, \Phi \in \Omega_1, y \in \left\{1,2,\dots,N_y\right\} \tag{10}$$

where N_i is the total number of type i resource; and $S_{y,i,j}$

equals 1 when the resource is developed, and 0 otherwise.

Considering the limited available investment capital each year, the annual investment budget is limited as:

$$\sum_i c_i^{inv} P_i\left(X_{i,y} - X_{i,y-1}\right) \le INV_y \tag{11}$$

where INV_y is the investment limit in year y; and c_i^{inv} is the investment cost per unit capacity of type i resource.

In the context of decarbonization, governments typically issue policies setting green power development targets, one of which is to specify the proportion of installed renewable energy capacity for each year.

$$\sum_{i \in \Omega_2} X_{i,y} P_i + \sum_{i \in \Omega_3} X_{i,y} P_i \ge \eta_y \left(\sum_{i \in \Omega_4} X_{i,y} P_i + \sum_{i \in \Omega_5} X_{i,y} P_i \right) \quad \forall y \in \left\{1, 2, ..., N_y\right\} \tag{12}$$

where η_y is the required installed renewable energy capacity in year y; and $\Omega_2 = \left\{\mathbb{N}_H, \mathbb{N}_W, \mathbb{N}_P\right\}$, $\Omega_3 = \left\{\mathbb{E}_H, \mathbb{E}_W, \mathbb{E}_P\right\}$, $\Omega_4 = \left\{\mathbb{N}_C, \mathbb{N}_G, \mathbb{N}_N, \mathbb{N}_H, \mathbb{N}_W, \mathbb{N}_P\right\}$, $\Omega_5 = \left\{\mathbb{E}_C, \mathbb{E}_G, \mathbb{E}_N, \mathbb{E}_H, \mathbb{E}_W, \mathbb{E}_P\right\}$, and $\mathbb{E}_C$, $\mathbb{E}_G$, $\mathbb{E}_N$, $\mathbb{E}_H$, $\mathbb{E}_W$, and $\mathbb{E}_P$ are the type sets of existing coal units, gas units, nuclear units, hydropower units, wind power units, and PV units, respectively.

B. Stage 2: UC of Operation Simulation

In Stage 2, the UC of operation simulation is conducted on a time scale of one hour. The variables involved in this stage are the operation statuses, including the startup and shutdown statuses of generators, the charging and discharging statuses of energy storage units, and the regulation status of DR loads. The costs incurred in this stage C_{S2} include the startup and shutdown costs of generators, expressed as:

$$C_{S2} = \sum_{y=1}^{N_y} \sum_{s=1}^{N_s} \sum_{i \in \Phi_G} \sum_{j=1}^{N_{i,y}} \sum_{t=1}^{N_t} \gamma_y \frac{N_d}{N_s} \left[c_i^{su} I_{y,s,i,j,t} \left(1 - I_{y,s,i,j,t-1}\right) + c_i^{sd} I_{y,s,i,j,t-1} \left(1 - I_{y,s,i,j,t}\right) \right] \tag{13}$$

where $I_{y,s,i,j,t}$ is the operation status of the j^{th} type i generator on typical day s in year y, which equals 1 in the startup status and 0 in the shutdown status; Φ_G is the type set of generators with startup-shutdown costs; c_i^{su} and c_i^{sd} are the startup and shutdown costs of generator, respectively; $N_{i,y}$ is the number of generators in year y; N_s is the total number of typical days in a year, indexed by s; N_t is the number of dispatch cycles in the operation simulation, indexed by t; and N_d is the total number of days in a year. While the cost in (13) is a summation of costs, the underlying optimization problem is dynamic. This is because the unit status variables are governed by inter-temporal constraints that link the decisions at time t to the system status at time $t-1$.

The constraints for the optimization in Stage 2 are all related to the operation statuses of units, including the startup/shutdown constraints of generators, the charging and discharging constraints of energy storage units, and the status constraints of DR loads.

For an existing generator, its operation status $I_{y,s,i,j,t}$ satisfies:

$$0 \le I_{y,s,i,j,t} \le 1 \quad \forall i \in \Phi, \Phi \in \Omega_6 \tag{14}$$

where $\Omega_6 = \left\{\mathbb{E}_C, \mathbb{E}_G, \mathbb{E}_N\right\}$.

For a newly developed generator, its operation status $I_{y,s,i,j,t}$ is subject to its development status $S_{y,i,j}$, which is expressed as:

$$0 \le I_{y,s,i,j,t} \le S_{y,i,j} \quad \forall i \in \Phi, \Phi \in \Omega_7 \tag{15}$$

where $\Omega_7 = \left\{\mathbb{N}_C, \mathbb{N}_G, \mathbb{N}_N\right\}$.

For energy storage units, the charging and discharging statuses are mutually exclusive, expressed as:

$$I_{y,s,i,j,t}^{ch} + I_{y,s,i,j,t}^{dis} \le 1 \quad \forall i \in \Phi, \Phi \in \left\{\mathbb{E}_S, \mathbb{N}_S\right\} \tag{16}$$

where $I_{y,s,i,j,t}^{dis}$ and $I_{y,s,i,j,t}^{ch}$ are the binary variables used to indicate charging and discharging statuses of energy storage units, respectively; and $\mathbb{E}_S$ is the type set of existing energy storage units. And for the existing and newly developed energy storage units, their statuses are constrained by (17) and (18), respectively.

$$\begin{cases} 0 \le I_{y,s,i,j,t}^{ch} \le 1 \\ 0 \le I_{y,s,i,j,t}^{dis} \le 1 \end{cases} \quad \forall i \in \mathbb{E}_S \tag{17}$$

$$\begin{cases} 0 \le I_{y,s,i,j,t}^{ch} \le S_{y,i,j} \\ 0 \le I_{y,s,i,j,t}^{dis} \le S_{y,i,j} \end{cases} \quad \forall i \in \mathbb{N}_S \tag{18}$$

For DR loads, the statuses of power reduction and increase are mutually exclusive, expressed as:

$$I_{y,s,i,j,t}^{inc} + I_{y,s,i,j,t}^{red} \le 1 \quad \forall i \in \Phi, \Phi \in \left\{\mathbb{E}_D, \mathbb{N}_D\right\} \tag{19}$$

where $I_{y,s,i,j,t}^{inc}$ and $I_{y,s,i,j,t}^{red}$ are the binary variables used to indicate the statuses of power reduction and increase, respectively; and $\mathbb{E}_D$ is the type set of existing DR loads. And for the existing and newly developed DR loads, their statuses are constrained by (20) and (21), respectively.

$$\begin{cases} 0 \le I_{y,s,i,j,t}^{inc} \le 1 \\ 0 \le I_{y,s,i,j,t}^{red} \le 1 \end{cases} \quad \forall i \in \mathbb{E}_D \tag{20}$$

$$\begin{cases} 0 \le I_{y,s,i,j,t}^{inc} \le S_{y,i,j} \\ 0 \le I_{y,s,i,j,t}^{red} \le S_{y,i,j} \end{cases} \quad \forall i \in \mathbb{N}_D \tag{21}$$

C. Stage 3: Power Dispatch of Operation Simulation

In Stage 3, the power dispatch of operation simulation is conducted on a time scale of one hour. The variables involved in this stage are the power of units, including the output power of generators, the charging and discharging power of energy storage units, and the response power of DR loads. The costs incurred in this stage C_{S3} are the variable operation and maintenance (VOM) costs, including the fuel costs of coal, gas, and nuclear units $C_{y,s}^{fuel}$, the discharging and charging costs of energy storage units $C_{y,s}^{S}$, the response costs of DR loads $C_{y,s}^{D}$, the costs of carbon emissions $C_{y,s}^{CO_2}$, and the costs of penalties for renewable energy curtailment and load loss $C_{y,s}^{P}$, expressed as:

$$C_{S3} = \sum_{y=1}^{N_y} \gamma_y \frac{N_d}{N_s} \sum_{s=1}^{N_s} \left(C_{y,s}^{fuel} + C_{y,s}^{S} + C_{y,s}^{D} + C_{y,s}^{CO_2} + C_{y,s}^{P} \right) \tag{22}$$

$$C_{y,s}^{fuel} = \sum_{\Phi \in \Omega_8} \sum_{i \in \Phi} \sum_{j=1}^{N_{i,y}} \sum_{t=1}^{N_t} \left(b_i P_{y,s,i,j,t} + c_i \right) \tag{23}$$

$$C_{y,s}^{S} = \sum_{i \in \left\{\mathbb{N}_S, \mathbb{E}_S\right\}} \sum_{j=1}^{N_{i,y}} \sum_{t=1}^{N_t} \left(c_i^{dis} P_{y,s,i,j,t}^{dis} + c_i^{ch} P_{y,s,i,j,t}^{ch} \right) \tag{24}$$

$$C_{y,s}^{D}=\sum_{i\in\{\mathbb{N}_D,\mathbb{E}_D\}}\sum_{j=1}^{N_{i,y}}\sum_{t=1}^{N_t}\left(c^{red}P_{y,s,i,j,t}^{red}+c^{inc}P_{y,s,i,j,t}^{inc}\right) \tag{25}$$

$$C_{y,s}^{CO_2}=\sum_{\Phi\in\Omega_9}\sum_{i\in\Phi}\sum_{j=1}^{N_{i,y}}\sum_{t=1}^{N_t}c_i^{CO_2}P_{y,s,i,j,t} \tag{26}$$

$$C_{y,s}^{P}=\sum_{t=1}^{N_t}\left(c_1^{p}P_{y,s,t}^{p1}+c_2^{p}P_{y,s,t}^{p2}\right) \tag{27}$$

where b_i and c_i are the fuel cost coefficients of generator; $P_{y,s,i,j,t}$ is the power of generator; $P_{y,s,i,j,t}^{ch}$ and $P_{y,s,i,j,t}^{dis}$ are the charging and discharging power of energy storage unit, respectively; c_i^{ch} and c_i^{dis} are the charging and discharging cost coefficients of energy storage unit, respectively; $P_{y,s,i,j,t}^{red}$ and $P_{y,s,i,j,t}^{inc}$ are the power reduction and increase of DR loads, respectively; c^{red} and c^{inc} are the cost coefficients of load reduction and increase, respectively; $c_i^{CO_2}$ is the cost coefficient of carbon emission; $P_{y,s,t}^{p1}$ and $P_{y,s,t}^{p2}$ are the load loss power due to power shortage and the wind and PV power curtailment due to power excess, respectively, and c_1^p and c_2^p are their penalty costs; $\Omega_8=\{\mathbb{E}_C,\mathbb{E}_G,\mathbb{E}_N,\mathbb{N}_C,\mathbb{N}_G,\mathbb{N}_N\}$; and $\Omega_9=\{\mathbb{E}_C,\mathbb{E}_G,\mathbb{N}_C,\mathbb{N}_G\}$.

In this stage, constraints that need to be followed include carbon emission reduction path constraints, power supply constraints, energy storage unit constraints, DR load constraints, and power system operation constraints.

1) Carbon Emission Reduction Path Constraints

In order to recommend the low-carbon development of the power system, governments develop carbon emission reduction paths. Thus, the carbon emissions from generation for each year in the operation simulation need to comply with the constraints of the given path.

$$\sum_{\Phi\in\Omega_9}\sum_{i\in\Phi}\frac{N_d}{N_s}\sum_{s=1}^{N_s}\sum_{j=1}^{N_{i,y}}\sum_{t=1}^{N_t}CE_i\cdot P_{y,s,i,j,t}\le CEL_y\quad\forall y\in\{1,2,...,N_y\} \tag{28}$$

where CE_i is the carbon emission coefficient of type i resource; and CEL_y is the carbon emission limit in year y.

2) Power Supply Constraints

Power supply constraints include constraints on conventional generators, renewable energy units, and external power supply. The operation of conventional generators is subject to performance limitations. The output constraint (29) limits their power, and the ramp constraint (30) limits their power change rate.

$$\begin{aligned}&I_{y,s,i,j,t}P_{i,\min}\le P_{y,s,i,j,t}\le I_{y,s,i,j,t}P_{i,\max}\quad\forall i\in\Phi,\Phi\in\Omega_8,\\&y\in\{1,2,\dots,N_y\},s\in\{1,2,\dots,N_s\},t\in\{2,3,\dots,N_t\}\end{aligned} \tag{29}$$

$$R_{i,\min}\le P_{y,s,i,j,t}-P_{y,s,i,j,t-1}\le R_{i,\max} \tag{30}$$

where $P_{i,\max}$ and $P_{i,\min}$ are the upper and lower limits of the output of generator, respectively; and $R_{i,\max}$ and $R_{i,\min}$ are the ramp up rate and ramp down rate limits of generator, respectively.

Considering the uncertainty in renewable energy generation, its output is constrained within a box uncertainty set determined based on historical data.

The constraint for wind power generation is shown in (31).

$$P_{y,s,i,j,t}^{W}=\hat{P}_{y,s,i,j,t}^{W}\left(1+\Delta P_{y,s,i,j,t}^{W}\right)\quad\Delta P_{\min}^{W}\le\Delta P_{y,s,i,j,t}^{W}\le\Delta P_{\max}^{W} \tag{31}$$

where $\hat{P}_{y,s,i,j,t}^{W}$ is the predicted wind power output; and $\Delta P_{y,s,i,j,t}^{W}$ is the uncertainty deviation of wind power caused by the prediction error, and $\Delta P_{\max}^{W}$ and $\Delta P_{\min}^{W}$ are the maximum and minimum values of this deviation, respectively.

The constraint for PV power generation is shown in (32).

$$P_{y,s,i,j,t}^{P}=\hat{P}_{y,s,i,j,t}^{P}\left(1+\Delta P_{y,s,i,j,t}^{P}\right)\quad\Delta P_{\min}^{P}\le\Delta P_{y,s,i,j,t}^{P}\le\Delta P_{\max}^{P} \tag{32}$$

where $\hat{P}_{y,s,i,j,t}^{P}$ is the predicted PV power output; and $\Delta P_{y,s,i,j,t}^{P}$ is the uncertainty deviation of PV power caused by the prediction error, and $\Delta P_{\max}^{P}$ and $\Delta P_{\min}^{P}$ are the maximum and minimum values of this deviation, respectively.

The external power input to the region via transmission lines also has uncertainty, constrained with a boxed uncertainty set in (33).

$$P_{y,s,i,t}^{E}=\hat{P}_{y,s,i,t}^{E}\left(1+\Delta P_{y,s,i,t}^{E}\right)\quad P_{\min}^{E}\le\Delta P_{y,s,i,t}^{E}\le\Delta P_{\max}^{E} \tag{33}$$

where $\hat{P}_{y,s,i,t}^{E}$ is the predicted value of external power; and $\Delta P_{y,s,i,t}^{E}$ is the uncertainty deviation of external power, and $\Delta P_{\max}^{E}$ and $\Delta P_{\min}^{E}$ are the maximum and minimum values of this deviation, respectively.

3) Energy Storage Unit Constraints

The discharging and charging power limits of energy storage units are shown in (34) and (35), respectively. The power stored in the energy storage unit is constrained by the capacity limits, as shown in (36). Meanwhile, the initial and ending electricity stocks of each energy storage unit are kept equal in the one-day operation simulation, as shown in (37).

$$0\le P_{y,s,i,j,t}^{dis}\le I_{y,s,i,j,t}^{dis}P_{i,\max}^{dis} \tag{34}$$

$$0\le P_{y,s,i,j,t}^{ch}\le I_{y,s,i,j,t}^{ch}P_{i,\max}^{ch} \tag{35}$$

$$E_{i,\min}\le E_{i,j,0}+\eta_{ch}\sum_{\tau=1}^{t}P_{y,s,i,j,\tau}^{ch}-\eta_{dis}\sum_{\tau=1}^{t}P_{y,s,i,j,\tau}^{dis}\le E_{i,\max} \tag{36}$$

$$\eta_{dis}\sum_{t=1}^{N_t}P_{y,s,i,j,t}^{dis}-\eta_{ch}\sum_{t=1}^{N_t}P_{y,s,i,j,t}^{ch}=0\quad\forall i\in\Phi,\Phi\in\{\mathbb{E}_S,\mathbb{N}_S\} \tag{37}$$

where $P_{i,\max}^{dis}$ and $P_{i,\max}^{ch}$ are the maximum discharging and charging power of energy storage unit, respectively; η_{dis} and η_{ch} are the discharging and charging efficiencies of energy storage unit, respectively; $E_{i,\min}$ and $E_{i,\max}$ are the minimum and maximum power that can be stored by the energy storage unit, respectively; and $E_{i,j,0}$ is the initial power stored in the energy storage unit.

4) DR Load Constraints

The reduced and increased power limits of DR loads are shown in (38) and (39), respectively.

$$0\le P_{y,s,i,j,t}^{inc}\le I_{y,s,i,j,t}^{inc}\left(P_{i,j,\max}^{load}-P_{i,j,t}^{load}\right) \tag{38}$$

$$0\le P_{y,s,i,j,t}^{red}\le I_{y,s,i,j,t}^{red}\left(P_{y,s,i,j,t}^{load}-P_{i,j,\min}^{load}\right)\quad\forall i\in\Phi,\Phi\in\{\mathbb{E}_D,\mathbb{N}_D\} \tag{39}$$

where $P_{i,j,\max}^{load}$ and $P_{i,j,\min}^{load}$ are the upper and lower limits of the DR load power $P_{i,j,t}^{load}$, respectively.

Adjustable DR loads can reduce or increase their power consumption over a period of time depending on the demand of power system. The regulation of load power in one time period does not affect the load power in other time periods. Adjustable DR loads only need to satisfy constraints (38) and (39), while transferable loads need to satisfy more than them. The regulated power of transferable loads in one time period needs to be reversed in other time periods to keep the overall electricity consumption of the load at a constant value. Therefore, the transferable DR loads need to satisfy the additional constraint expressed as:

$$\sum_{t=1}^{N_t}\left(P^{red}_{y,s,i,j,t}-P^{inc}_{y,s,i,j,t}\right)=0 \tag{40}$$

5) Power System Operation Constraints

Power system operation constraints include power balance constraints and reserve constraints. The power balance constraints ensure that the power generated is equal to the power consumed at each moment, expressed as:

$$\begin{aligned}&\sum_{\Phi\in\Omega_8}\sum_{i\in\Phi}\sum_{j=1}^{N_{i,y}}P_{y,s,i,j,t}+\sum_{\Phi\in\{\mathbb{E}_S,\mathbb{N}_S\}}\sum_{i\in\Phi}\sum_{j=1}^{N_{i,y}}\left(P^{dis}_{y,s,i,j,t}-P^{ch}_{y,s,i,j,t}\right)+P^W_{y,s,t}+\\&P^P_{y,s,t}+P^E_{y,s,t}=P^{load}_{y,s,t}+\sum_{\Phi\in\{\mathbb{E}_D,\mathbb{N}_D\}}\sum_{i\in\Phi}\sum_{j=1}^{N_{i,y}}\left(P^{inc}_{y,s,i,j,t}-P^{red}_{y,s,i,j,t}\right)\\&\forall y\in\{1,2,\ldots,N_y\},s\in\{1,2,\ldots,N_s\},t\in\{1,2,\ldots,N_t\}\end{aligned} \tag{41}$$

where $P^{load}_{y,s,t}$, $P^W_{y,s,t}$, $P^P_{y,s,t}$, and $P^E_{y,s,t}$ are the total load power, wind power, PV power, and external power, respectively. $P^W_{y,s,t}$, $P^P_{y,s,t}$, and $P^E_{y,s,t}$ are calculated by (42)-(44), respectively.

$$P^W_{y,s,t}=\sum_{\Phi\in\{\mathbb{E}_W,\mathbb{N}_W\}}\sum_{i\in\Phi}\sum_{j=1}^{N_i}P^W_{y,s,i,j,t} \tag{42}$$

$$P^P_{y,s,t}=\sum_{\Phi\in\{\mathbb{E}_P,\mathbb{N}_P\}}\sum_{i\in\Phi}\sum_{j=1}^{N_i}P^P_{y,s,i,j,t} \tag{43}$$

$$P^E_{y,s,t}=\sum_{\Phi\in\{\mathbb{E}_E,\mathbb{N}_E\}}\sum_{i\in\Phi}\sum_{j=1}^{N_i}P^E_{y,s,i,t} \tag{44}$$

where $P^W_{y,s,i,j,t}$ and $P^P_{y,s,i,j,t}$ are the power of a single wind power unit and PV unit, respectively; and $P^E_{y,s,i,t}$ is the power transmitted on a single external source.

The power reserve constraints are further divided into up and down reserve constraints, as shown in (45) and (46), respectively.

$$\begin{aligned}&\sum_{\Phi\in\boldsymbol{\Omega}_8}\sum_{i\in\Phi}\sum_{j=1}^{X_{i,y}}\left(P_{i,\max}I_{y,s,i,j,t}-P_{i,y,s,t}\right)+\\&\sum_{\Phi\in\{\mathbb{E}_S,\mathbb{N}_S\}}\sum_{i\in\Phi}\sum_{j=1}^{N_{i,y}}\left(P^{ch}_{y,s,i,j,t}-P^{dis}_{y,s,i,j,t}+P^{dis}_{i,j,\max}\right)+\\&\sum_{\Phi\in\{\mathbb{E}_D,\mathbb{N}_D\}}\sum_{i\in\Phi}\sum_{j=1}^{X_{i,y}}\left(P^{load}_{y,s,i,j,t}+P^{inc}_{y,s,i,j,t}-P^{red}_{y,s,i,j,t}-P^{load}_{i,j,\min}\right)+\\&\Delta P^W_{y,s,t}+\Delta P^P_{y,s,t}+\Delta P^E_{y,s,t}\geq\rho_u P^{load}_{y,s,t}\\&\forall y\in\{1,2,\ldots,N_y\},s\in\{1,2,\ldots,N_s\},t\in\{1,2,\ldots,N_t\}\end{aligned} \tag{45}$$

$$\begin{aligned}&\sum_{\Phi\in\boldsymbol{\Omega}_8}\sum_{i\in\Phi}\sum_{j=1}^{X_{i,y}}\left(P_{i,y,s,t}-P_{i,\min}I_{y,s,i,j,t}\right)+\\&\sum_{\Phi\in\{\mathbb{E}_S,\mathbb{N}_S\}}\sum_{i\in\Phi}\sum_{j=1}^{X_{i,y}}\left(P^{ch}_{i,j,\max}-P^{ch}_{y,s,i,j,t}+P^{dis}_{y,s,i,j,t}\right)+\\&\sum_{\Phi\in\{\mathbb{E}_D,\mathbb{N}_D\}}\sum_{i\in\Phi}\sum_{j=1}^{X_{i,y}}\left(P^{load}_{i,j,\max}-P^{load}_{y,s,i,j,t}-P^{inc}_{y,s,i,j,t}+P^{red}_{y,s,i,j,t}\right)-\\&\Delta P^W_{y,s,t}-\Delta P^P_{y,s,t}-\Delta P^E_{y,s,t}\geq\rho_d P^{load}_{y,s,t}\\&\forall y\in\{1,2,\ldots,N_y\},s\in\{1,2,\ldots,N_s\},t\in\{1,2,\ldots,N_t\}\end{aligned} \tag{46}$$

where $\Delta P^W_{y,s,t}$, $\Delta P^P_{y,s,t}$, and $\Delta P^E_{y,s,t}$ are the differences between the actual value and the predicted value for total wind power, PV power, and external power, respectively; and ρ_u and ρ_d are the up and down reserve coefficients, respectively.

D. Three-stage Robust Planning Model

The above three stages are combined and incorporated into the robust optimization technology to form a three-stage robust planning model. The overall objective function of this model is to minimize the total cost of the power system over the planning period, as shown in (47). The overall constraints combine the constraints for each of the three stages, which are (8)-(12), (14)-(21), and (28)-(46).

$$\min_{\boldsymbol{X}}\left(C_{S1}+\min_{\boldsymbol{I}\in\Omega(\boldsymbol{X})}\left(C_{S2}+\max_{\boldsymbol{u}\in\boldsymbol{U}}\min_{\boldsymbol{P}\in\Psi(\boldsymbol{I},\boldsymbol{u})}C_{S3}\right)\right) \tag{47}$$

In Stage 1, the decision variable is the number of resources to be developed $\boldsymbol{X}$. The planning model decides on an optimal investment portfolio to minimize the development and FOM costs C_{S1}, anticipating all future operational possibilities. In Stage 2, the decision variable is the resource status $\boldsymbol{I}$. Given the built assets, the planning model determines the resource status $\boldsymbol{I}$ to minimize the startup and shutdown costs C_{S2} before intraday uncertainties are known. In Stage 3, the decision variable is the resource power $\boldsymbol{P}$. The planning model reveals the worst-case uncertainty $\boldsymbol{u}$ that maximizes operation costs. Facing this worst-case scenario, it determines the optimal intraday power to minimize variable costs C_{S3}.These three stages are critically interdependent. The resource status $\boldsymbol{I}$ to be developed is constrained by $\boldsymbol{X}$, denoted as $\boldsymbol{I}\in\Omega(\boldsymbol{X})$. And the resource power $\boldsymbol{P}$ is constrained by the resource status $\boldsymbol{I}$ and worst-case uncertainty $\boldsymbol{u}$, denoted as $\boldsymbol{P}\in\Psi(\boldsymbol{I},\boldsymbol{u})$. The decisions from the above three stages, which occur on different timescales, are mathematically coupled within a single hierarchical framework to form the three-stage robust planning model. This integration ensures that the long-term investment decisions are optimized while accounting for their future operation consequences.

IV. Solution Algorithm for Three-stage Robust Planning Model

Integrating the first two stages involving integer variables, the above three-stage robust planning model for low-carbon transition pathway of power system can be organized into the following compact form.

$$\begin{cases}\min\limits_{\boldsymbol{X},\boldsymbol{I}}\left(\boldsymbol{a}^{\mathrm{T}}\boldsymbol{X}+\boldsymbol{b}^{\mathrm{T}}\boldsymbol{I}+\max\limits_{\boldsymbol{u}\in\boldsymbol{U}}\min\limits_{\boldsymbol{P}\in\Psi(\boldsymbol{I},\boldsymbol{u})}\boldsymbol{c}^{\mathrm{T}}\boldsymbol{P}\right)\\ \text{s.t. }\boldsymbol{AX}\geq\boldsymbol{d}\\ \quad\boldsymbol{X}+\boldsymbol{BS}=\boldsymbol{0}\\ \quad\boldsymbol{CS}+\boldsymbol{DI}\geq\boldsymbol{g}\\ \quad\boldsymbol{EI}+\boldsymbol{FP}+\boldsymbol{G}^E\boldsymbol{u}^E+\boldsymbol{G}^N\boldsymbol{u}^N\geq\boldsymbol{h}\\ \quad\boldsymbol{RP}=\boldsymbol{r}\\ \quad\boldsymbol{u}^E\in\boldsymbol{U}^E\\ \quad\boldsymbol{u}^N\in\boldsymbol{U}^N\end{cases} \tag{48}$$

where $\boldsymbol{S}$ is the optimization variable, denoting the resource development status; $\boldsymbol{a}$, $\boldsymbol{b}$, and $\boldsymbol{c}$ are the column vectors of cost coefficients; $\boldsymbol{A}$, $\boldsymbol{B}$, $\boldsymbol{C}$, $\boldsymbol{D}$, $\boldsymbol{E}$, $\boldsymbol{F}$, $\boldsymbol{G}^E$, $\boldsymbol{G}^N$, and $\boldsymbol{R}$ are the coefficient matrices; $\boldsymbol{d}$, $\boldsymbol{g}$, $\boldsymbol{h}$, and $\boldsymbol{r}$ are the constant column vectors; and $\boldsymbol{u}^E$ and $\boldsymbol{u}^N$ are the uncertain variables with E and N denoting existed resources and resources to be developed, respectively, and $\boldsymbol{U}^E$ and $\boldsymbol{U}^N$ are their corresponding uncertain sets. In (48), the first constraint corresponds to (8), (9), (11), and (12). The second constraint corresponds to (10). The third constraint corresponds to (14) - (21). The fourth constraint corresponds to (28) - (36), (38), (39), and (42)-(46). The fifth constraint corresponds to (37) and (40).

A key feature of this model is the presence of decision-dependent uncertainty. Specifically, the investment decisions $\boldsymbol{S}$ in Stage 1 determine whether newly developed renewable resources are built, which in turn defines the uncertainty set for their power output $\boldsymbol{u}^N$ in Stage 3. Standard decomposition algorithms such as the traditional CCG algorithm are predicated on a fixed and static uncertainty set and cannot be directly applied to solve this model. To address this challenge, the CCG algorithm is modified as MCCG algorithm. This algorithm is ideologically consistent with the traditional CCG algorithm, decomposing the original problem into master problem and subproblem. The master problem solves the development scheme and UC scheme, while the subproblem finds the worst-case scenario that maximizes the minimum value of the operation cost for a given development and start/stop scenario. The master problem and subproblem are solved alternately to obtain the lower and upper bounds on the objective function of the original problem. Variables and constraints related to the worst-case scenario obtained in the subproblem are continuously introduced to the master problem during the solution process to obtain more compact lower bounds on the value of the original objective function. The final converged values of the upper and lower bounds are the optimal solution of the original problem. The core modification of the MCCG algorithm is the ability to dynamically construct the uncertainty set of subproblem at each iteration based on the investment decisions passed from the master problem.

The master problem obtained by decomposing the original problem is denoted as:

$$\begin{cases} \min f_{MP}=\min\limits_{\boldsymbol{X},\boldsymbol{I},\boldsymbol{P}_l}\left(\boldsymbol{a}^{\mathrm{T}}\boldsymbol{X}+\boldsymbol{b}^{\mathrm{T}}\boldsymbol{I}+\theta\right) \\ \text{s.t. } \theta\geq \boldsymbol{c}^{\mathrm{T}}\boldsymbol{P}_l \\ \quad \boldsymbol{AX}\geq \boldsymbol{d} \\ \quad \boldsymbol{X}+\boldsymbol{BS}=\boldsymbol{0} \\ \quad \boldsymbol{CS}+\boldsymbol{DI}\geq \boldsymbol{g} \\ \quad \boldsymbol{DS}+\boldsymbol{EI}+\boldsymbol{FP}_l+\boldsymbol{G}^E\boldsymbol{u}_l^{E*}+\boldsymbol{G}^N\boldsymbol{u}_l^{N*}\geq \boldsymbol{h} \\ \quad \boldsymbol{RP}_l=\boldsymbol{r} \quad \forall l\in\mathbb{N}^+\bigcap l\leq k \end{cases} \tag{49}$$

where θ is the cutting plane; k is the index of current iterations; l is a positive integer less than or equal to k; $\boldsymbol{P}_l$ is the vector of variables added in iteration l; and $\boldsymbol{u}_l^{E*}$ and $\boldsymbol{u}_l^{N*}$ are the uncertain variables in the master problem in iteration l, as shown in (50) and (51), respectively, with * denoting the optimal variables. Their values in the worst-case scenario obtained from the subproblem in the previous iteration are used, and their values taken in the initial iteration are given manually.

$$\boldsymbol{u}_l^{E*}=\left[\boldsymbol{P}_l^{load*},\boldsymbol{P}_l^{E_W*},\boldsymbol{P}_l^{E_P*},\boldsymbol{P}_l^{E_E*}\right]^{\mathrm{T}} \tag{50}$$

$$\boldsymbol{u}_l^{N*}=[\boldsymbol{P}_l^{N_W*}\odot\boldsymbol{S}^{N_W},\boldsymbol{P}_l^{N_P*}\odot\boldsymbol{S}^{N_P},\boldsymbol{P}_l^{N_E*}\odot\boldsymbol{S}^{N_E}]^{\mathrm{T}} \tag{51}$$

where $\odot$ is the symbol of Hadamard product; the superscripts $load$, E_W, E_P, and E_E represent the load, existing wind power, existing PV power, and external power, respectively; and the superscripts N_W, N_P, and N_E represent the wind power, PV power, and external power to be developed, respectively.

The subproblem in iteration k obtained by decomposing the original problem is denoted as:

$$\begin{cases} \max\limits_{\boldsymbol{u}}\min\limits_{\boldsymbol{P}}\left(\boldsymbol{c}^{\mathrm{T}}\boldsymbol{P}+\boldsymbol{a}^{\mathrm{T}}\boldsymbol{X}_k^*+\boldsymbol{b}^{\mathrm{T}}\boldsymbol{I}_k^*\right) \\ \text{s.t. } \boldsymbol{DS}_k^*+\boldsymbol{EI}_k^*+\boldsymbol{FP}+\boldsymbol{G}^E\boldsymbol{u}^E+\boldsymbol{G}^N\boldsymbol{u}^N\geq \boldsymbol{h} \\ \quad \boldsymbol{RP}=\boldsymbol{r} \\ \quad \boldsymbol{u}^E\in \boldsymbol{U}^E \\ \quad \boldsymbol{u}^N\in \boldsymbol{U}_k^{N*} \end{cases} \tag{52}$$

where $\boldsymbol{I}_k^*$ is the optimal variable of resource operation obtained by solving the master problem in iteration k; and $\boldsymbol{U}_k^{N*}$ is the uncertain power output set for the resources to be developed determined in the master problem, as shown in (53).

$$\begin{aligned} \boldsymbol{U}_k^{N*}=\Big\{&\boldsymbol{u}^N=\left[\boldsymbol{P}^{N_W},\boldsymbol{P}^{N_P},\boldsymbol{P}^{N_E}\right]^{\mathrm{T}}, \\ &\boldsymbol{P}^{N_W}\in\left[1+\Delta\boldsymbol{P}_{\min}^{N_W},1+\Delta\boldsymbol{P}_{\max}^{N_W}\right]\odot\hat{\boldsymbol{P}}^{N_W}\odot\boldsymbol{S}_k^{N_W*}, \\ &\boldsymbol{P}^{N_P}\in\left[1+\Delta\boldsymbol{P}_{\min}^{N_P},1+\Delta\boldsymbol{P}_{\max}^{N_P}\right]\odot\hat{\boldsymbol{P}}^{N_P}\odot\boldsymbol{S}_k^{N_P*}, \\ &\boldsymbol{P}^{N_E}\in\left[1+\Delta\boldsymbol{P}_{\min}^{N_E},1+\Delta\boldsymbol{P}_{\max}^{N_E}\right]\odot\hat{\boldsymbol{P}}^{N_E}\odot\boldsymbol{S}_k^{N_E*}\Big\} \end{aligned} \tag{53}$$

where $\hat{\boldsymbol{P}}$ is the vector of predicted power; and $\Delta\boldsymbol{P}_{\min}$ and $\Delta\boldsymbol{P}_{\max}$ are the vectors of the minimum and maximum power deviations, respectively.

The subproblem is a two-layer optimization problem, which can be transformed into a single-layer optimization by transforming the inner optimization problem into KKT conditions as shown in (54).

$$\begin{cases} \max f_{SP}=\max\limits_{\boldsymbol{u},\boldsymbol{P}}\left(\boldsymbol{c}^{\mathrm{T}}\boldsymbol{P}+\boldsymbol{a}^{\mathrm{T}}\boldsymbol{X}_k^*+\boldsymbol{b}^{\mathrm{T}}\boldsymbol{I}_k^*\right) \\ \text{s.t. } \boldsymbol{c}^{\mathrm{T}}-\boldsymbol{F\lambda}-\boldsymbol{R\mu}=\boldsymbol{0} \\ \quad \boldsymbol{EI}_k^*+\boldsymbol{FP}+\boldsymbol{G}^E\boldsymbol{u}^E+\boldsymbol{G}^N\boldsymbol{u}^N\geq \boldsymbol{h} \\ \quad \left(\boldsymbol{h}-\boldsymbol{EI}_k^*-\boldsymbol{FP}-\boldsymbol{G}^E\boldsymbol{u}^E-\boldsymbol{G}^N\boldsymbol{u}^N\right)\boldsymbol{\lambda}=\boldsymbol{0} \\ \quad \boldsymbol{RP}=\boldsymbol{r} \\ \quad \boldsymbol{\lambda}\geq\boldsymbol{0} \\ \quad \boldsymbol{u}^E\in \boldsymbol{U}^E \\ \quad \boldsymbol{u}^N\in \boldsymbol{U}_k^{N*} \end{cases} \tag{54}$$

where $\boldsymbol{\lambda}$ is the Lagrange multiplier corresponding to the constraint $\boldsymbol{EI}_k^*+\boldsymbol{FP}+\boldsymbol{G}^E\boldsymbol{u}^E+\boldsymbol{G}^N\boldsymbol{u}^N\geq \boldsymbol{h}$; and $\boldsymbol{\mu}$ is the Lagrange multiplier of the constraint $\boldsymbol{RP}=\boldsymbol{r}$.

After the above derivations and transformations, the proposed robust planning model is finally decoupled into the master problem (49) and the subproblem (54) in the mixed-integer linear form, which can be subsequently solved by the MCCG algorithm with the following procedure.

Step 1: give a set of uncertain variables $\boldsymbol{u}_1^{E*}$ and $\boldsymbol{u}_1^{N*}$ as the initial worst-case scenario, set the lower and upper bounds of the optimal objective value of the original problem as $LB=-\infty$ and $UB=+\infty$, and set the number of iterations $k=1$.

Step 2: according to the worst-case scenario $\boldsymbol{u}_l^{E*}$ and $\boldsymbol{u}_l^{N*}$ for $\forall l \in \mathbb{N}^+ \bigcap l \le k$, solve the master problem (49) to obtain the optimal objective value $\left(f_{MP}\right)_k^*$ and the optimal values of the corresponding variables $\boldsymbol{X}_k^*, \boldsymbol{S}_k^*, \boldsymbol{I}_k^*, \theta_k^*, \boldsymbol{P}_1^*, \ldots, \boldsymbol{P}_k^*$. Update the lower bound $LB=\max\left\{LB, \left(f_{MP}\right)_k^*\right\}$ of the objective function of the original problem.

Step 3: solve the subproblem by substituting the obtained solutions $\boldsymbol{X}_k^*$, $\boldsymbol{S}_k^*$, and $\boldsymbol{I}_k^*$ of the master problem into (54) to obtain the optimal objective function value $\left(f_{SP}\right)_k^*$ of the subproblem and the corresponding value of the uncertain variable $\boldsymbol{u}$ in the worst-case scenario $\boldsymbol{u}_{k+1}^{E*}$ and $\boldsymbol{u}_{k+1}^{N*}$. Update the upper bound of the objective function of the original problem $UB=\min\left\{UB, \left(f_{SP}\right)_k^*\right\}$.

Step 4: set the convergence threshold ε of the algorithm. If $UB-LB \le \varepsilon \cdot LB$, then stop the iteration and return to the optimal solution $\boldsymbol{X}_k^*$, $\boldsymbol{S}_k^*$, $\boldsymbol{I}_k^*$, and $\boldsymbol{P}_k^*$; otherwise, add variable $\boldsymbol{P}_{k+1}$ to the master problem and the following constraints. Let $k=k+1$ and jump to *Step 2* until the algorithm converges.

$$\begin{cases} \theta \ge \boldsymbol{c}^{\mathrm{T}} \boldsymbol{P}_{k+1} \\ \boldsymbol{EI} + \boldsymbol{FP}_{k+1} + \boldsymbol{G}^E \boldsymbol{u}_{k+1}^{E*} + \boldsymbol{G}^N \boldsymbol{u}_{k+1}^{N*} \ge \boldsymbol{h} \\ \boldsymbol{RP}_{k+1} = \boldsymbol{r} \end{cases} \tag{55}$$

V. CASE STUDY

In this section, a provincial power system in eastern China is modified as an example to conduct the low-carbon transition pathway planning during the period of 2025-2050. The planning is based on the current status of this power system, with some data sourced from [40]. The peak load and electricity forecasts and carbon emission targets during the period of 2025-2050 are shown in Supplementary Material A Table SAI, referenced and modified from [16]. The operation costs of DR loads are hypothetical as shown in Supplementary Material A Table SAII according to multiple studies [41]-[45]. The simulation is carried out based on the Sim-CPSS platform of NARI Group.

A. Planning in Different Scenarios

This subsection employs the three scenarios previously established, which involve investment cost changes driven by learning effects influenced by policies. They are advanced scenario with faster rate of decline, moderate scenario with medium rate of decline, and conservative scenario with slower rate of decline. The data on investment costs for various types of resources are obtained from NREL [38], as shown in Supplementary Material A Fig. SA1. The learning rates of DR technology are taken as 15%, 10%, and 5% in the advanced, moderate, and conservative scenarios, respectively.

The installed capacity of newly developed resource in 2025-2050 in the three scenarios is shown in Fig. 3.

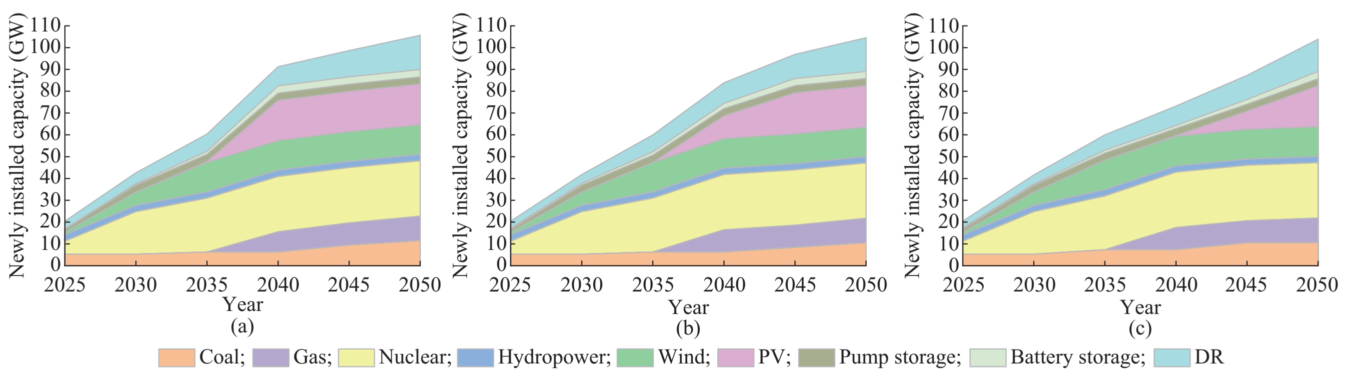

Fig. 3. Installed capacity of newly developed resource in 2025-2050 in three scenarios. (a) Advanced scenario. (b) Moderate scenario. (c) Conservative scenario.

It can be seen that the advanced scenario has the largest installed capacity of PV and wind power until 2040. Subsequently, the installed capacity in the moderate and conservative scenarios decreases in that order. This is due to the fact that the investment costs fall faster in the advanced scenario, making wind power and PV power become more economical generation sources. Therefore, in the advanced scenario, the system prioritizes investments in wind power units and PV units at an earlier stage. And after 2045, when the renewable energy sources have been fully developed, the number of sources in all three scenarios reaches the upper limit and no longer makes a difference. This demonstrates that the proactive policies and high learning rates promote the development of renewable energy sources during the mid-development period.

Over the development of the system, the investment cost of DR loads decreases based on different learning rates. The cumulative installed capacity of developed DR loads and investment cost changing ratio over time are shown in Fig. 4.

As shown in Fig. 4, the scenarios with higher learning rates lead to higher investment in DR capacity, which in turn accelerates the cost decline. This result is consistent with our theory. The present discounted values (PDVs) of costs in the advanced, moderate, and conservative scenarios are shown in Supplementary Material A Fig. SA2, which increase sequentially and are 741, 749, and 772 million CNY, respectively. This increasement is mainly caused by the investment costs, while the FOM costs and VOM costs change little. It can be concluded that a higher learning rate contributes to lowering the overall cost of the system, which aligns with the realities of social development.

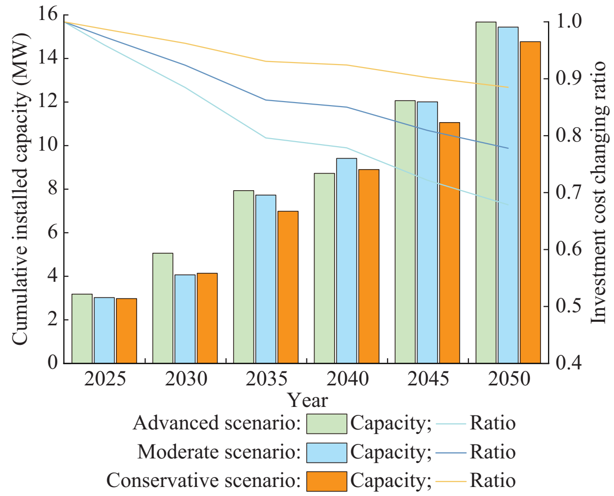

Fig. 4. Cumulative installed capacity of developed DR load and investment cost changing ratio over time.

B. Impact of DR Loads on Planning Results

Based on the learning rate of the moderate scenario, the results of planning with and without considering DR loads are compared. The installed capacity of newly developed resource without considering DR loads is shown in Fig. 5.

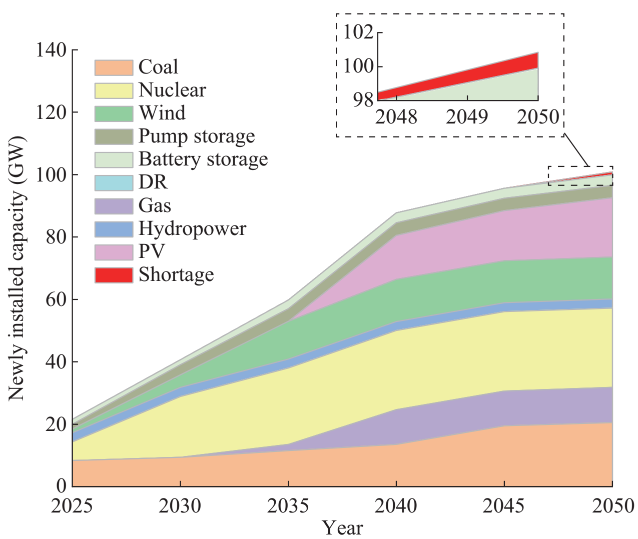

Fig. 5. Installed capacity of newly developed resource without considering DR loads.

Compared with the case considering DR loads in Fig. 3(b), in the case without considering DR loads, the development of wind power units is delayed, more coal units are developed in each year, and the development of energy storage units is brought forward. Specifically, the installed capacity of wind power units is 2 GW and 1.4 GW less in 2030 and 2035, respectively, and does not equalize until 2040 in the case without considering DR loads. This is mainly because the absence of DR loads leads to limited smoothing of wind power fluctuation. To address this problem, on the one hand, more energy storage units are developed in each year to provide fluctuation smoothing capabilities. On the other hand, units without fluctuation are developed to replace renewable energy generation, although they are more expensive. Benefitting from less peak loads and less stringent carbon emission constraints in the earlier few years of the planning period, more coal units are developed. For the final result in 2050, the coal units, gas units, and energy storage units to be developed are 10 GW, 1.1 GW, and 2.8 GW more, respectively. The total costs increase by 11.9 billion CNY, with investment costs and FOM costs increasing by 18 billion CNY, startup and shutdown costs increasing by 1 billion CNY, and VOM costs decreasing by 7.1 billion CNY. The decrease in VOM costs is mainly due to the replacement of costly DR loads with cheaper generators. This demonstrates the positive role of DR loads in integrating renewable energy and reducing the total costs of power system.

The capacity of the DR load with different operation cost multipliers, taking the data in Supplementary Material A Table SAII as the base value, is shown in Supplementary Material A Fig. SA3. The difference in capacity with different operation costs is mainly observed in the later few years of the planning period. That is, the difference is small in 2025-2035 and large in 2040-2050. Further analysis is performed from the perspective of system operation. Figure 6 shows how the system allocates DR loads to either power regulation or as a operation reserve at different cost points, demonstrating that the role of DR loads changes as their economic viability varies. It can be seen that in the early years of planning period, DR loads are mainly used as operation reserve, and gradually participate in system operation regulation in the later years. The reason for this phenomenon is that DR loads have low investment costs but high operation costs. For DR loads to be an economical flexible resource to utilize its regulation capability, it should have an operation cost of 40% its baseline value or less. As the years go by, the carbon constraints and fluctuation of renewable energy generation make it possible for more expensive DR loads to participate in the system operation regulation. By 2050, DR load with 5 times the VOM cost will also be partially involved in system operation regulation.

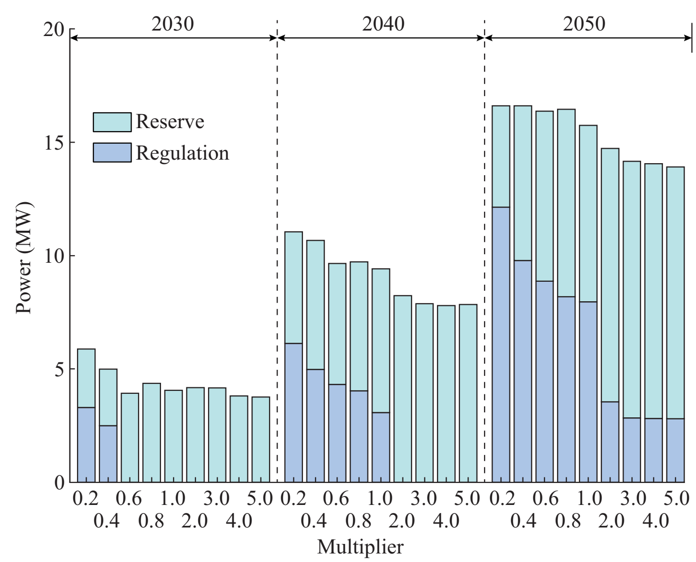

Fig. 6. Role of DR loads with different operation cost multipliers

C. Effect Comparison of Three-stage and Two-stage Models

To demonstrate the technoeconomic advantages, we conduct a comparative analysis between our three-stage robust model and a conventional two-stage robust optimization model, which is commonly used in the existing literature. The two-stage model simplifies the planning problem by omitting the intermediate UC stage, thereby neglecting start-up/shutdown costs and constraints. This comparison aims to quantify the necessity of incorporating a dedicated UC stage for ensuring the economic efficiency and operation reliability of the long-term plan. The differences between the planning cases with and without UC are compared in the moderate scenario. The planning result obtained by the two-stage model is shown in Fig. 7. Compared with the planning results of the proposed model, the development of coal units is significantly reduced and replaced with gas units. The development of wind power units is earlier and increases in number. And the total costs rise by 28.6 billion CNY.

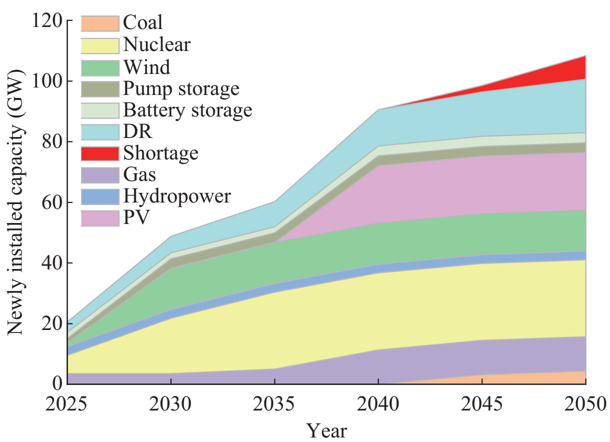

Fig. 7. Planning results obtained by two-stage model.

The reasons for this phenomenon are examined by comparing unit operating conditions in the two cases. Supplementary Material A Fig. SA4(a) and (b) presents the unit output and CO_2 emission intensity curves for a typical spring day in 2050, with and without UC, respectively. In spring, the lower loads and higher PV and wind power outputs mean that the coal, gas, and nuclear units do not all need to start when UC is applied. When PV generation is low, the operating units supply power at higher outputs; when PV generation increases, the operating units reduce their outputs accordingly. Without UC, however, all units must start up. Due to low load levels, they mainly operate at the minimum output, and when PV generation is high, they cannot shut down, causing power oversupply. The surplus is absorbed by energy storage units and released at night, avoiding PV curtailment but increasing operating costs. Coal generation in Fig. SA4(b) is notably higher than that in Fig. SA4(a), especially from 10:00 to 17:00, leading to greater carbon emissions—116.48 kg more per typical spring day without UC. Supplementary Material A Fig. SA4(c) and (d) shows similar results for a typical summer day in 2050. Because carbon emissions during low load periods (e.g., spring) are excessive and difficult to offset, allowable emissions during peak hours in summer are constrained, limiting coal unit output. Consequently, the system relies more on expensive resources such as DR loads to maintain balance. When flexible resources are exhausted in the evening, the load curtailment occurs, with the largest loss at 22:00 reaching 7.78 GW, causing significant penalty costs.

It can be observed that determining the UC prior to the optimal dispatch of power system can effectively improve the flexibility of power system and has the effect of reducing the cost and carbon emission of the system operation during low load periods. Therefore, it is necessary to consider UC in operation simulations during the planning process and establish a three-stage planning model, especially for future power systems with high penetration of renewable energy.

VI. Conclusion

In this paper, a robust planning framework of power system decarbonization pathway is developed. In the framework, the influence of social factors such as government policies on planning is considered in terms of investment cost changes and system development constraints to ensure that the planning results align with social development needs. DR loads as important flexible resources are also considered to cope with the uncertainty and fluctuation associated with high penetration of renewable energy. To obtain a planning scheme that enables the system to operate safely, economically, and stably even under the worst uncertainties, a novel three-stage robust planning model integrating operation simulation including UC stage is proposed. And a tailored MCCG algorithm is proposed to solve this model with inherent decision-dependent uncertainties. Case studies demonstrate that the flexibility of DR loads plays a positive role in enabling the large-scale integration of renewable energy into power systems and reducing system development and operational costs, thereby effectively advancing the low-carbon transition of power system. A comparative analysis against a conventional two-stage robust optimization model demonstrates that the three-stage model is not only more cost-effective with lower total system costs, but also essential for operation reliability, avoiding significant load shedding events, proving it a superior model for planning the decarbonization of power systems.

References

[1] UN Environment Program. (2022, Oct.). Emissions Gap Report 2022 [Online]. Available: http://www.unep.org/resources/emissions-gap-report-2022

[2] S. Zhou, Q. Tong, X. Pan *et al.*, "Research on low-carbon energy transformation of China necessary to achieve the Paris agreement goals: a global perspective," *Energy Economics*, vol. 95, p. 105137, Mar. 2021.

[3] China Electricity Council. (2023, Jul.). Annual Development Report of China Electric Power Industry 2023. [Online]. Available: https://cec.org.cn/detail/index.html?3-322625

[4] Y. Xue and X. Yu, "Beyond smart grid: cyber–physical–social system in energy future," *Proceedings of the IEEE*, vol. 105, no. 12, pp. 2290-2292, Dec. 2017.

[5] M. J. B. Kabeyi and O. A. Olanrewaju, "Sustainable energy transition for renewable and low carbon grid electricity generation and supply," *Frontiers in Energy Research*, vol. 9, p. 743114, Mar. 2022.

[6] B. Kroposki, "Integrating high levels of variable renewable energy into electric power systems," *Journal of Modern Power Systems and Clean Energy*, vol. 5, no. 6, pp. 831-837, Nov. 2017.
[7] C. Vrionis, V. Tsalavoutis, and A. Tolis, "A generation expansion planning model for integrating high shares of renewable energy: a meta-model assisted evolutionary algorithm approach," *Applied Energy*, vol. 259, p. 114085, Feb. 2020.
[8] I. A. Khan, H. Mokhlis, N. N. Mansor *et al*., "New trends and future directions in load frequency control and flexible power system: a comprehensive review," *Alexandria Engineering Journal*, vol. 71, pp. 263-308, May 2023.
[9] G. G. Dranka, P. Ferreira, and A. I. F. Vaz, "Integrating supply and demand-side management in renewable-based energy systems," *Energy*, vol. 232, p. 120978, Oct. 2021.
[10] S. Chen, P. Liu, and Z. Li, "Low carbon transition pathway of power sector with high penetration of renewable energy," *Renewable and Sustainable Energy Reviews*, vol. 130, p. 109985, Sept. 2020.
[11] T. Zang, S. Wang, Z. Wang *et al*., "Integrated planning and operation dispatching of source–grid–load–storage in a new power system: a coupled socio–cyber–physical perspective," *Energies*, vol. 17, no. 12, p. 3013, Jun. 2024.
[12] N. Zhang, Z. Hu, B. Shen *et al*., "A source–grid–load coordinated power planning model considering the integration of wind power generation," *Applied Energy*, vol. 168, pp. 13-24, Apr. 2016.
[13] J. K. Delson and S. M. Shahidehpour, "Linear programming applications to power system economics, planning and operations," *IEEE Transactions on Power Systems*, vol. 7, no. 3, pp. 1155-1163, Aug. 1992.
[14] S. Majumdar and D. Chattopadhyay, "A model for integrated analysis of generation capacity expansion and financial planning," *IEEE Transactions on Power Systems*, vol. 14, no. 2, pp. 466-471, May 1999.
[15] E. D. Delarue, P. J. Luickx, and W. D. D'haeseleer, "The actual effect of wind power on overall electricity generation costs and CO_2 emissions," *Energy Conversion and Management*, vol. 50, no. 6, pp. 1450-1456, Jun. 2009.
[16] S. Luo, W. Hu, W. Liu *et al*., "Transition pathways towards a deep decarbonization energy system: a case study in Sichuan, China," *Applied Energy*, vol. 302, p. 117507, Nov. 2021.
[17] R. Xie, W. Wei, M. Li *et al*., "Sizing capacities of renewable generation, transmission, and energy storage for low-carbon power systems: a distributionally robust optimization approach," *Energy*, vol. 263, p. 125653, Jan. 2023.
[18] G. Pan, Z. Gu, Y. Sun *et al*., "Multi-stage provincial power expansion planning and multi-market trading equilibrium," *Journal of Modern Power Systems and Clean Energy*, vol. 12, no. 5, pp. 1652-1665, Sept. 2024.
[19] Y. Chen, L. He, J. Li *et al*., "An inexact bi-level simulation-optimization model for conjunctive regional renewable energy planning and air pollution control for electric power generation systems," *Applied Energy*, vol. 183, pp. 969-983, Dec. 2016.
[20] V. Asgharian, M. M. A. Abdelaziz, and I. Kamwa, "Multi-stage bi-level linear model for low carbon expansion planning of multi-area power systems," *IET Generation*, *Transmission & Distribution*, vol. 13, no. 1, pp. 9-20, Jan. 2019.
[21] M. A. El-Meligy and A. M. El-Sherbeeny, "Hybrid robust/stochastic transmission expansion planning considering uncertainties in generators' offer prices: a second-order cone program approach," *Electric Power Systems Research*, vol. 203, p. 107631, Feb. 2022.
[22] N. Zhang, H. Jiang, E. Du *et al*., "An efficient power system planning model considering year-round hourly operation simulation," *IEEE Transactions on Power Systems*, vol. 37, no. 6, pp. 4925-4935, Nov. 2022.
[23] S. Y. Abujarad, M. W. Mustafa, and J. J. Jamian, "Recent approaches of unit commitment in the presence of intermittent renewable energy resources: a review," *Renewable and Sustainable Energy Reviews*, vol. 70, pp. 215-223, Apr. 2017.
[24] S. Wang, C. Zhao, L. Fan *et al*., "Distributionally robust unit commitment with flexible generation resources considering renewable energy uncertainty," *IEEE Transactions on Power Systems*, vol. 37, no. 6, pp. 4179-4190, Nov. 2022.
[25] K. Choubineh, H. Yousefi, and M. Moeini-Aghtaie, "Developing a new flexibility-oriented model for generation expansion planning studies of renewable-based energy systems," *Energy Reports*, vol. 11, pp. 706-719, Jun. 2024.
[26] K. Marti, *Stochastic Optimization Methods: Applications in Engineering and Operations Research*. Cham: Springer International Publishing, 2024.
[27] A. Ben-Tal and A. Nemirovski, "Robust optimization – methodology and applications," *Mathematical Programming*, vol. 92, no. 3, pp. 453-480, May 2002.
[28] B. Zeng and L. Zhao, "Solving two-stage robust optimization problems using a column-and-constraint generation method," *Operations Research Letters*, vol. 41, no. 5, pp. 457-461, Sept. 2013.
[29] B. Zeng and W. Wang. (2022, Mar.). Two-stage robust optimization with decision dependent uncertainty. [Online]. Available: https://arxiv.org/abs/2203.16484
[30] K. J. Arrow, "The economic implications of learning by doing," *The Review of Economic Studies*, vol. 29, no. 3, p. 155, Jun. 1962.
[31] E. Williams, E. Hittinger, R. Carvalho *et al*., "Wind power costs expected to decrease due to technological progress," *Energy Policy*, vol. 106, pp. 427-435, Jul. 2017.
[32] S. Hong, Y. Chung, and C. Woo, "Scenario analysis for estimating the learning rate of photovoltaic power generation based on learning curve theory in South Korea," *Energy*, vol. 79, pp. 80-89, Jan. 2015.
[33] W. R. Stewart and K. Shirvan, "Capital cost estimation for advanced nuclear power plants," *Renewable and Sustainable Energy Reviews*, vol. 155, p. 111880, Mar. 2022.
[34] M. Junginger, E. Hittinger, E. Williams *et al*., *Technological Learning in the Transition to a Low-carbon Energy System*, New York: Academic Press, 2020.
[35] Y. Zhou and A. Gu, "Learning curve analysis of wind power and photovoltaics technology in US: cost reduction and the importance of research, development and demonstration," *Sustainability*, vol. 11, no. 8, p. 2310, Apr. 2019.
[36] J. C. Goldschmidt, L. Wagner, R. Pietzcker *et al*., "Technological learning for resource efficient terawatt scale photovoltaics," *Energy & Environmental Science*, vol. 14, no. 10, pp. 5147-5160, Sept. 2021.
[37] M. D. Carelli, P. Garrone, G. Locatelli *et al*., "Economic features of integral, modular, small-to-medium size reactors," *Progress in Nuclear Energy*, vol. 52, no. 4, pp. 403-414, May 2010.
[38] NREL. (2022, Jan.). Annual Technology Baseline Workbook 2022. [Online]. Available: https://atb.nrel.gov/electricity/2022/data
[39] L. Chen, G. Msigwa, M. Yang *et al*., "Strategies to achieve a carbon neutral society: a review," *Environmental Chemistry Letters*, vol. 20, no. 4, pp. 2277-2310, Apr. 2022.
[40] People's Government of Zhejiang Province. (2021, Jan.). Zhejiang Province Electricity Development Fourteen Five Plan. [Online]. Available: http://minyi.zjzwfw.gov.cn/dczjnewls/dczj/idea/topic_2828.html
[41] F. Elghitani and W. Zhuang, "Aggregating a large number of residential appliances for demand response applications," *IEEE Transactions on Smart Grid*, vol. 9, no. 5, pp. 5092-5100, Sept. 2018.
[42] S. I. Vagropoulos, G. A. Balaskas, and A. G. Bakirtzis, "An investigation of plug-in electric vehicle charging impact on power systems scheduling and energy costs," *IEEE Transactions on Power Systems*, vol. 32, no. 3, pp. 1902-1912, May 2017.
[43] S. A. Mansouri, M. S. Javadi, A. Ahmarinejad *et al*., "A coordinated energy management framework for industrial, residential and commercial energy hubs considering demand response programs," *Sustainable Energy Technologies and Assessments*, vol. 47, p. 101376, Oct. 2021.
[44] People's Government of Anhui Province. (2025, Jun.). Notice on the Issuance of the Anhui Province Electricity Demand Response Implementation Plan. [Online]. Available: https://www.ahjd.gov.cn/Jczwgk/show/3553986.html
[45] People's Government of Zhejiang Province. (2025, Jun.). Notice from the Zhejiang Provincial Development and Reform Commission on Issuing the Implementation Plan for Demand Side Management of Electricity in Zhejiang Province during the Peak Summer of 2025. [Online]. Available: https://www.pvmeng.com/2025/06/04/40067

Haiyue Yu received the B.S. degree in electrical engineering from Shandong University, Jinan, China, in 2020. He is currently working toward the Ph.D. degree in electrical engineering at Zhejiang University, Hangzhou, China. His current research interests include power system planning and operation optimization integrating demand response technology.

Yusheng Xue received the Ph.D. degree from the University of Liege, Liege, Belgium, in 1987. He has been an Academician with the Chinese Academy of Engineering since 1995. He is currently the Honorary President of the State Grid Electric Power Research Institute (SGEPRI), Nanjing, China. He is the Editor-in-Chief of Automation of Electric Power Systems (in Chinese) and Journal of Modern Power Systems and Clean Energy, as well as the Chairman of the Technical Committee of Chinese National Commit-

tee of CIGRE since 2005. His research interest includes power system automation.

Minglei Bao received the B.S. degree in electrical engineering from Shandong University, Jinan, China, and the Ph.D. degree in electrical engineering from Zhejiang University, Hangzhou, China, in 2016 and 2021, respectively. He is currently an Assistant Researcher at Zhejiang University. His research interests include reliability analysis of integrated energy system, complex network, and electricity market.

Hengyu Hui received the B.Eng. and Ph.D. degrees in electrical engineering from Zhejiang University, Hangzhou, China, in 2019 and 2024, respectively. His research interests include operation of integrated energy system and demand response.

Dongliang Xie received the Ph.D. degree in electrical engineering from Southeast University, Nanjing, China, in 2012. During 2011-2012, he was a Research Associate in Hong Kong Polytechnic University, Hong Kong, China. He is currently working for State Grid Electric Power Research Institute (SGEPRI), Nanjing, China. His interests include analysis, simulation, and control for smart grid architectures and essentials consisting of renewable power generation.

Yi Ding received the B.S. and Ph.D. degrees in electrical engineering from Shanghai Jiao Tong University, Shanghai, China, and Nanyang Technological University, Singapore, in 2002 and 2007, respectively. He is a Professor with the College of Electrical Engineering, Zhejiang University, Hangzhou, China. His interests include power system analysis incorporating renewable energy source, smart grid performance analysis, and engineering system reliability modeling and optimization.